Letter

## Spin-incoherent liquid and interaction-driven criticality in the one-dimensional Hubbard model

Jia-Jia Luo , 1,2 Han Pu , 3,\* and Xi-Wen Guan , 1,4,5,†

<sup>1</sup>Innovation Academy for Precision Measurement Science and Technology, Chinese Academy of Sciences, Wuhan 430071, China <sup>2</sup>University of Chinese Academy of Sciences, Beijing 100049, China

<sup>3</sup>Department of Physics and Astronomy, and Rice Center for Quantum Materials, Rice University, Houston, Texas 77251-1892, USA

<sup>4</sup>NSFC-SPTP Peng Huanwu Center for Fundamental Theory, Xi'an 710127, China

(Received 7 September 2022; revised 7 February 2023; accepted 24 April 2023; published 4 May 2023)

Although the one-dimensional repulsive Fermi-Hubbard model has been intensively studied over many decades, a rigorous understanding of many aspects of the model is still lacking. In this work, based on the solutions to the thermodynamic Bethe ansatz equations, we provide a rigorous study on the following. (1) We calculate the fractional excitations of the system in various phases, from which we identify the parameter regime featuring the spin-incoherent Luttinger liquid (SILL). We investigate the universal properties and the asymptotic of correlation functions of the SILL. (2) We study the interaction-driven phase transition and the associated criticality, and build up an essential connection between the contact susceptibilities and the variations of density, magnetization, and entropy with respect to the interaction strength. As an application of these concepts, which hold true for higher-dimensional systems, we propose a quantum cooling scheme based on the interaction-driven refrigeration cycle.

DOI: 10.1103/PhysRevB.107.L201103

One-dimensional (1D) Fermi-Hubbard model, describing strongly correlated electrons in a 1D lattice, has become increasingly important in ultracold atoms, condensed matter, and quantum metrology. Owing to the Bethe ansatz exact solution of the model [1,2], a variety of strongly correlated many-body phenomena have been extensively studied for over 40 years, including Tomonaga-Luttinger liquid (TLL) [3–5], spin-charge separation [6-9], thermal and magnetic properties [10–16], the Fulde-Ferrell-Larkin-Ovchinnikov (FFLO) [17,18] pairing correlation [19-24], etc. On the experimental side, 1D exactly solvable models have been successfully realized in the laboratory, allowing us to compare elegant and sophisticated exact solutions directly with experimen-tal measurements [25-28], Significant new experimental developments cover a broad range of physics such as the generalized hydrodynamics [29-31], dynamical fermionization [32], TLL [33-35], fractional exclusion statistics [36], quantum holonomy [37,38], p-wave interacting fermions [39–41], high spin symmetry magnetism [42,43], etc.. For a recent review, see Ref. [44].

Despite these tremendous efforts, many aspects of the model still lack rigorous understanding. In particular, phase transitions have been extensively studied in the context of varying external potentials such as chemical potential and magnetic field. However, interaction-driven phase transitions have not received sufficient attention even though interaction plays an essential role in many-body systems. Although there are some previous studies along this line (see, for example,

Refs. [45–47]), the important quantum critical scaling functions for interaction-driven phase transitions have not been systematically studied. This can be attributed to the fact that interaction strength is hardly tunable in traditional solid materials. The advent of cold atoms completely changed this situation as interaction strengths in atomic systems have been routinely controlled via Feshbach resonance. A notable recent example is the demonstration of the spin-charge separation [48–52] in a 1D continuum Fermi gas where the spin and the charge velocities are shown to exhibit distinct dependence on the interaction strength [53].

Motivated by this, in this Letter, we show that the tunability of interaction strength allows further exploration of the spin-incoherent Luttinger liquid (SILL) [54–57] and interaction-driven quantum phase transitions in the Hubbard model. Specifically, we present rigorous results of fractional charge and spin excitations, analytical results on the asymptotic of single-particle Green's function and pair correlation functions of the SILL, and interaction-driven criticality. Furthermore, inspired by the notion of the partial wave contact in ultracold Fermi gas [58,59], we build up general relations between contact susceptibilities and the variation of density, magnetization, and entropy with respect to the interaction strength, using which we propose a quantum cooling scheme based on the interaction-driven refrigeration cycle.

1D Hubbard model. The 1D single-band Hubbard model is described by the Hamiltonian [1,5]

$$H = -t \frac{X^{L}}{(c_{j,a}^{\dagger}c_{j+1,a} + \text{H.c.}) + u} \frac{X^{L}}{(2n_{j,\uparrow} - 1)} \times (2n_{j,\downarrow} - 1) - \mu \hat{n} - 2B\hat{S}^{z},$$
 (1)

<sup>&</sup>lt;sup>5</sup>Department of Fundamental and Theoretical Physics, Research School of Physics, Australian National University, Canberra ACT 0200, Australia

<sup>\*</sup>hpu@rice.edu

<sup>†</sup>xiwen.guan@anu.edu.au

where  $c_{j,a}^{\dagger}$  ( $c_{j,a}$ ) is the creation (annihilation) operator of an electron with spin a ( $a = \uparrow$  or  $\downarrow$ ) at site j on a 1D lattice of length L, satisfying the standard anticommutation relations. t,  $\mu$ , and B are hopping amplitude, chemical potential, and magnetic field, respectively. In this work, we will only consider repulsive interaction with u > 0 and take t = 1 as the unit of the system.  $\mu$  and B are renormalized accordingly and become dimensionless. Meanwhile,  $n_{i,a} = c_i \dagger_n c_{i,a}$  and  $\hat{n}$  $n_{j,a}$  are the density operator and the average fermion  $n_{\underline{l}}^{\underline{l}}$  per lattice site, respectively. We denote the magnetization  $S^z = P(n_{j,\uparrow} - n_{j,\downarrow})/2$ . For vanishing external potentials  $(\mu = 0, {}^jB = 0)$  and even L, Hamiltonian (1) possesses  $SO(4) \boxtimes SU(2) \times SU(2)/Z_2$  symmetry, preserving spin rotational and  $\eta$ -pairing symmetries [5,60,61], i.e.,  $[H, S^{\alpha}] = 0 = [H, \eta^{\alpha}]$  with  $\alpha = x, y, z$ . The spin and  $\eta$ -pair operators can be transformed to each other via Shiba transformation, showing the connection between spin and charge [5]; also see the Supplemental Material (SM) [62]. We will use spin and  $\eta$ -pair magnetizations  $S^z$ ,  $\eta^z = {}^1(N-L)$  to characterize the fractional spin and charge excitations.

In 1968 Lieb and Wu [1] derived the BA equations for the 1D Hubbard model by means of Bethe's hypothesis [64]. Takahashi [65] later found the root patterns of the BA equations, i.e., real k, length-n 3 string (known as spinon bound state) composed of n spin-down electrons, length-m k-3 string containing m down-spin and m up-spin particles, which determine both the ground and the excited states of the model. Building on Takahashi's string hypothesis, and using the Yang-Yang method [66], one can obtain the thermodynamic Bethe ansatz (TBA) equations of the model [65] (for convenience, see [62]). In principle, all thermodynamic properties of the model can be obtained from the TBA. However, solving the infinite number of nonlinear integral TBA equations poses a tremendous theoretical challenge. Therefore, many impor-tant questions remain to be answered.

Low-temperature phase diagram and fractional excitations. A rich phase diagram of the 1D Hubbard model (1) in magnetic field-chemical potential plane can be obtained from either the BA or the TBA equations at zero temper-ature. We find that the dimensionless Wilson ratio (WR)  $R_{W}^{W} = \frac{4}{3} \left( \frac{n_k B}{\mu^B \beta} \right)^2 \frac{\chi_s}{C_V/T}, \text{ where } \chi_s \text{ is the spin susceptibility and } C$ the specific heat conveniently characterizes the TLLs.

 $R_{W}^{\chi} = \frac{4}{3} (\frac{\pi_{kB}}{\mu^{B}g})^2 \frac{\chi_s}{C_V/T}$ , where  $\chi_s$  is the spin susceptibility and  $C_V$  the specific heat, conveniently characterizes the TLLs. Here  $k_B$ ,  $\mu_B$ , and g are the Boltzmann constant, the Bohr magneton, and the Landé factor, respectively, which we set to be unity in our calculation. The value of the WR is temperature independent at low energy and exhibits a sudden change in the vicinities of the phase boundaries. Such a finite temperature feature naturally maps out the full phase diagram of the 1D repulsive Hubbard model at zero temperature, as we show in Fig. 1. Specifically, we observe that the values of the WR in Fig. 1 confirm the bosonization result [56] of  $R^{\chi_s} = 2v_c K_s/(v_s + v_c)$ , 2 and  $4K_s$  for the TLLs in Phase IV, II and  $V_s$ , respectively, where  $K_s$  is the Luttinger parameter for spin, and  $v_{c,s}$  are sound velocities for charge and spin, respectively. The WR is zero for phases I and III; see SM [62] for more details.

Figures 2(a) and 2(b) demonstrate excitations at zero magnetic field in charge and spin degrees of freedom near the half-filled lattice and the dilute limit, respectively. The

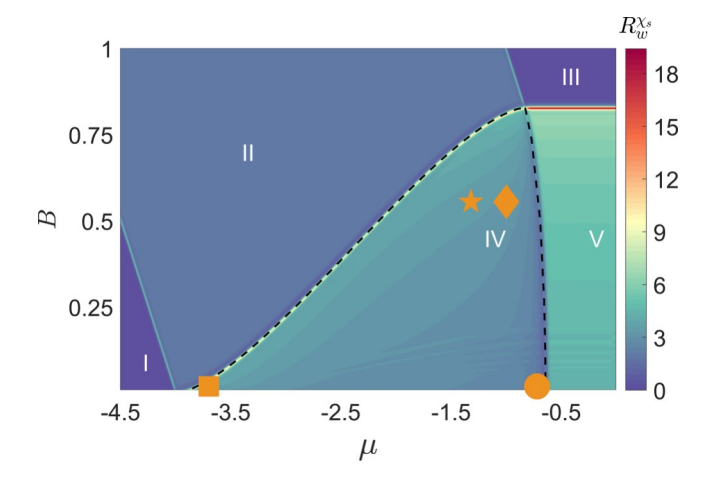


FIG. 1. Phase diagram represented by the contour plot of the Wilson ratio  $R_{K^{\circ}}$  at temperature T=0.005 and u=1. The corresponding phases are empty lattice I, partially filled and fully polarized phase II, fully filled and polarized phase III, partially filled and polarized phase IV, and fully filled and partially polarized phase V (Mott insulator). The dotted lines represent analytic solution of BA equations obtained at zero temperature. The orange symbols indicate the locations of excitations plotted in Fig. 2.

particle-hole excitation of charge (orange) forms continuum spectra within the first Brillouin zone. Flipping one spin leads to excitation spectrum (green) of two deconfined spinons with a fractional spin- $^1$ . In the long wavelength limit, i.e.,  $1K \rightarrow$ 

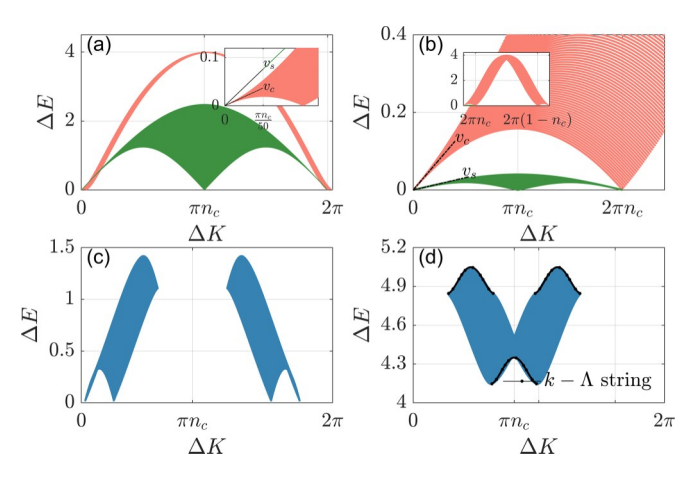


FIG. 2. Elementary fractional spin and charge excitations. The orange areas in (a) and (b) represent particle-hole excitations of charge, whereas the green parts show the two-spinon excitations with quantum numbers  $(1\eta^z, 1S^z) = (0, 1)$  induced from spin flipping. The inset in (a) shows the excitation for small momentum, while the inset in (b) shows the excitation for the momentum within the first Brillouin zone, whose zero energy modes are situated at  $0, 2\pi n_c, 2\pi(1-n_c), 2\pi$ . (c) Fractional antiholon-spinon excitations  $(\frac{1}{2}, -\frac{1}{2})$ , i.e., adding an extra spin-down electron to create an antiholon and a spinon. (d) Gapped excitation spectra for length-1 k-3 string and a length-2 3 string. All graphs are drawn in the first Brillouin zone with interaction u = 1 and the parameters (a)  $B = 0, \mu = -0.6619$ , density n = 0.9801 (near half-filled band), (b)  $B = 0, \mu = -3.8508$ , density n = 0.1389 (dilute limit), (c)  $B = 0.555, \mu = -1$ , and (d)  $B = 0.555, \mu = -1.32$ .

0, both charge and spin excitations exhibit linear dispersion:  $1E_{c,s} = v_{c,s} h |1K|$ , where  $v_c = 0.5995$ ,  $v_s = 1.2403$  in (a) and  $v_c = 0.7206$ ,  $v_s = 0.1454$  in (b), showing spin and charge separated excitations. However, subtle differences between these two limits are observed, i.e., for (a), the charge excitation displays a single-particle nature due to the vanishing of the charge Fermi sea; for (b), the spin and charge excitations are significantly separated, making this preferred region observe spin-charge separation [62]. Later, we will further demonstrate the existence of the SILL in region (b) for temperature  $E_s 
i k_B T 
i E_F$ , where  $E_{s,c} 
i k_F v_{s,c}$  with  $k_F = \pi n_c$  are the spin and charge energies, respectively. Figure 2(c) shows the fractional antiholon-spinon excitation spectra with the  $\eta$ -pair and spin magnetization  $(1\eta^z, 1S^z) = (\frac{1}{2}, -\frac{1}{2})$  by adding an antiholon particle  $N_e = N + 1$  superposed with one spinon particle in  $M_1$  sector, which is outside of the spin-charge separated TLL regime [62]. Figure 2(d) shows the two gapped excitations, i.e., length-1 k-3 string and length-2 3 spinon bound states, forming a gapped continuum band.

Universal scaling laws, SILL, and correlation functions. Rigorous results on quantum criticality of the repulsive Hubbard model remain largely unknown. At zero temperature, the phase transition occurs at a quantum critical point (QCP) where a degree of freedom appears, disappears, or reaches saturation. At finite temperature, the QCP fans out into the V-shaped quantum critical regime, in which the free energy takes universal form. By considering the relevant degrees of freedom, we can simplify the TBA equations and find such universal forms. In the SM [62], we have derived analytically the free energies of all quantum critical regions associated with various phase transitions of the 1D Hubbard model. Here, we only write down the free energy at quantum criticality for the II-IV and V-IV transitions:

$$f = f_0 - \frac{\pi T^2}{6v_c} + T^{\frac{3}{2}} \pi^{\frac{1}{2}} \sigma_1(0) \frac{\varepsilon_1^{00}(0)}{2}^{-\frac{1}{2}} \operatorname{Li}_{\frac{3}{2}}^{\frac{1}{2}} - e^{-\frac{\epsilon_{-(0)}}{T}}^{\frac{\epsilon_{-(0)}}{2}},$$

$$f = f_0 - \frac{\pi T^2}{6v_s} + T^{\frac{3}{2}} \pi^{\frac{1}{2}} \rho(\pi) \frac{\mu}{2} - \kappa^{\frac{\alpha}{2}} (\pi) \operatorname{Li}_{\frac{3}{2}}^{\frac{1}{2}} - e^{\frac{\kappa(\pi)}{T}}^{\frac{\epsilon_{-(0)}}{T}},$$
(2)

where  $\operatorname{Li}_n$  denotes the polylog functions,  $f_0$  is the ground-state energy, the  $T^2$  terms represent the contributions from the collective excitations of the background degree of freedom near the QCP,  $\sigma_1(0)$  denotes the spin density at 3 = 0,  $\varepsilon_1(3)$  is the dressed energy of length-1 string,  $\varepsilon^{00}(0) \equiv \frac{d^2 \varepsilon_1}{dt} |_{\frac{3-0}{dt}} \rho(\pi)$  denotes the charge density at  $k = \pi$ , and  $\kappa$   $(\pi) \equiv \frac{d^2 \varepsilon_1}{dt} |_{k=\pi}$ , with

$$\varepsilon_1(0) = -\alpha_B 1B - \alpha_\mu 1\mu - \alpha_u 1u,$$
  

$$\kappa(\pi) = \beta_B 1B + \beta_\mu 1\mu + \beta_u 1u$$
(3)

denoting the charge and spin dressed energy gaps away from the QCP, where  $1B = B - B_c$ ,  $1\mu = \mu - \mu_c$ , and  $1u = u - u_c$  are distances away from the QCP ( $B_c$ ,  $\mu_c$ ,  $u_c$ ). The analytic expressions of the factors  $\alpha_{B,\mu,u}$  are rather cumbersome and can be found in the SM [62]. As we will show below, the free energy in Eq. (2) elegantly leads to and provides a rigorous understanding of the universal thermodynamic properties of the TLL, the SILL, and the quantum scaling laws at criticality.

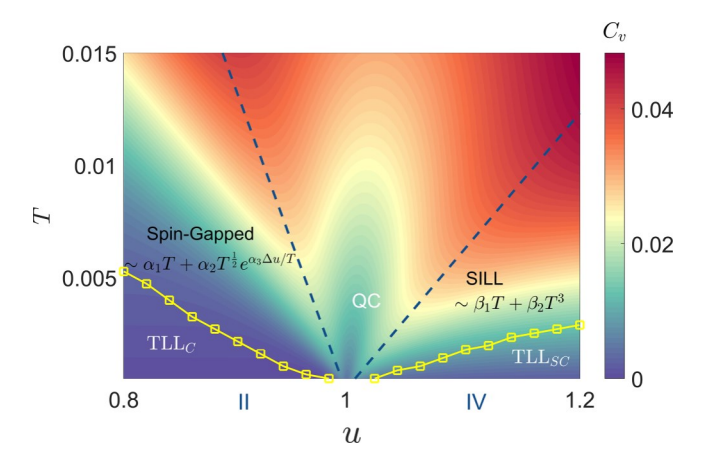


FIG. 3. Contour plot of specific heat in the T-u plane at  $\mu = -2$ , B = 0.55 for II-IV transition. The blue dashed lines present the critical temperatures determined by the maximum values of the specific heat [Eq. (4)]. The yellow lines with square symbols mark the TLL phase boundary, below which the specific heat shows a linear temperature dependence. Crossover regimes between the blue dashed and the yellow lines denote the spin-gapped phase (on the left) and the SILL phase (on the right).

In the quantum critical regime,  $T \ \lambda \ 1u$ , and from Eq. (2), the specific heat can be readily derived as

$$C_{\nu}/T = c_0 + c_1 T^{-1/2} \frac{f}{4} \operatorname{Li}_{\frac{3}{2}}(-e^x) - x \operatorname{Li}_{\frac{1}{2}}(-e^x) + x^2 \operatorname{Li}_{\frac{1}{2}}(-e^x) + O((1u/T)^{5/2}),$$
(4)

where  $x \equiv \alpha_u 1u/T$  and  $c_{0,1}$  denote the regular part and a constant depending on the critical point  $u_c$ , respectively. In Fig. 3, we display the contour plot of the specific heat in the plane spanned by T and u at  $\mu = -2$ , B = 0.55. The specific heat shows a bimodal structure, whose local maxima mark the crossover temperatures. The local maxima can be determined by  $\partial C_v/\partial u = 0$ , leading to  $x_1 = -1.5629$  and  $x_2 = 3.6205$ , corresponding to the two blue dashed lines in Fig. 3. These two lines join at  $u_c = 1$  at T = 0 and the quantum criti-cal regime resides between them, displaying a universal free fermion criticality, i.e., dynamical and correlation critical exponents Z = 2, v = 1/2, respectively.

In the SILL regime, the spin excitation is suppressed and hence the spin sector is nondynamic, while charge maintains relevant at low energy. Taking the reasonable limits  $|x \pm iv_c t|$   $\stackrel{?}{\leftarrow} v_c/T$  and  $|x \pm iv_s t|$   $\stackrel{?}{\wedge} v_s/T$ , we can calculate the finite-temperature single-particle Green's function and pair correlation function

$$G^{\uparrow} \approx e^{-i} k^{F,\uparrow x} C_{\uparrow}^{-}(x - iv_{c}t) h S_{R}^{+}(x, t) S_{R}(0, 0) i + \text{H.c.},$$

$$G_{p} \approx e^{-i} (k^{F,\uparrow +} k^{F,\downarrow})^{x} C_{p}^{-}(x - iv_{c}t) C_{p}^{+}(x + iv_{c}t)$$

$$\times h S_{R}^{+}(x, t) S_{R}(0, 0) i + \text{H.c.},$$
(5)

where the charge correlations  $C_{\uparrow}^{-}(Z) \, \mathbb{P} \, 1/Z^{21_c^+}$ ,  $C_p^{\pm}(Z) \, \mathbb{P} \, 1/Z^{21_c^+}$  decay as a power law of distance, whereas the spin mode correlation  $h_R^{S^+}(x,t) S_R(0,0)$  i  $(2\pi\alpha k_F)^{21_s^++21_s^-} e^{-\pi\alpha(21_s^++21_s^-)k_F x}$  decays exponentially. Here  $1_c^{\pm}$  are the conformal dimensions which can be calculated analytically and numerically [62];  $\alpha$  is a constant. For the particular case B=0, our results agree with those given in Ref. [57]. We comment that the SILL has been theoretically studied under the framework of bosonization [55–57]. Our work here provides a rigorous underpinning of the SILL based on the TBA.

Contact susceptibilities and quantum cooling. In analogy to the contact for quantum gases [58,59], here we define the lattice version of the coptact  $C = \partial f/\partial u = 4d - 2n + 1$ , where  $n = h\hat{n}i$ , and  $d = \frac{1}{N}$   $_ihn_{i,\uparrow}n_{i,\downarrow}i$  is the average double occupancy, a quantity which can also depict the phase diagram [62]. It is, however, more essential to define contact susceptibilities with respect to the external potentials. Using the Maxwell relations, we may build up general relations between contact susceptibilities and interaction-driven variations of entropy, density, and magnetization [62]:

$$\frac{\partial s}{\partial u} = -\frac{\partial C}{\partial T}, \quad \frac{\partial n}{\partial u} = -\frac{\partial C}{\partial \mu}, \quad \frac{\partial m}{\partial u} = -\frac{\partial C}{\partial (2B)}.$$
 (6)

These relations provide deep insights into the interaction effects and universal behavior of phase transitions.

As a specific example, we now use the first relation in Eqs. (6) to investigate interaction-driven quantum cooling. Figure 4(a) shows a contour plot of entropy in the T-u plane for fixed B and  $\mu$ . The interaction-driven phase transitions from I to II, II to IV, and IV to V occur sequentially with increasing interaction strength. We observe a single-component charge  $TLL_C$  in II, a spin and charge separated  $TLL_{SC}$  in IV, and a spin TLLs in the Mott phase V. Conducting the total derivative of entropy with respect to the interaction u, the phase points on the isentropic line in the T-u plane admit  $T \partial_u C_v = \partial_T \partial_T \partial_T \partial_C$  Thus the interaction-driven the relation Grüneisen parameter [67] defined by  $O_{int} = u \partial C$  quantifies the efficiency of interaction-driven refrigeration? Near a critical point, local maximum of the entropy leads to a local temperature minimum in an isentropic process and, using the condition  ${}^{\theta}_{C} = 0$ , we have  ${}^{1}\text{Li}_{1}(-e^{x}) - x \text{Li}_{-1}(-e^{x}) =$ 0, which give  $\overline{\xi}^T$  a general solution  $x \equiv : \alpha_u 1u/T \approx 1.3117$ . Using the free energy Eq. (2), we can obtain the explicit expression of the maximum entropy near the transition point from II to IV  $s_{c1} \approx \lambda_1 \pi^{1/2} \sigma_1(0) [\varepsilon^{00}(0)/2]^{-1/2} T^{1/2}$ , where  $\lambda_1 = x \operatorname{Li}_{1/2}(-e^x) - 3/2 \operatorname{Li}_{3/2}(-e^x) = 1.3467$ . Similarly, for phase transition from the Mott phase V to the phase IV, the maximum entropy is given by  $s \approx$  $\lambda_1 \pi^{1/2} \rho(\pi) [-\kappa^{00}(\pi)/2]^{-1/2} T^{1/2}$ . On the other hand, <sup>c2</sup>the

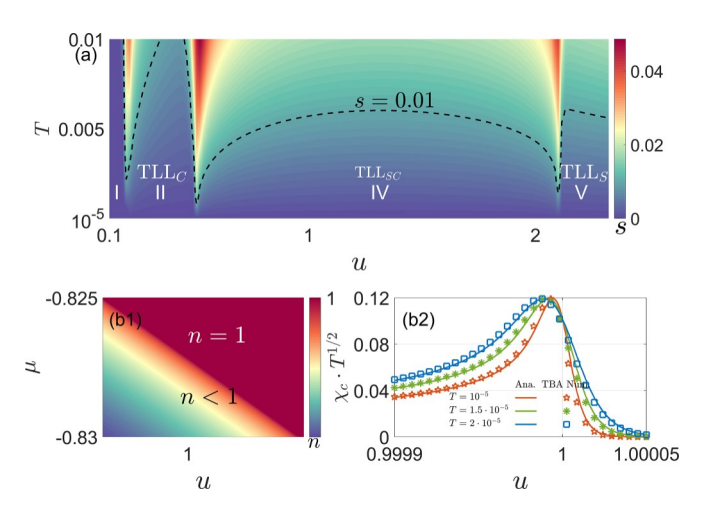


FIG. 4. (a) Contour plot of the entropy in the T-u plane for B=0.15,  $\mu=-2.5$ . Black dotted curve is the isentropic line for s=0.01. When the interaction increases, the system enters sequentially into phases II, IV, and V. (b1) Contour plot of density n near the IV-V phase transition with u=1,  $\mu=-0.82724$ , and  $B_c=0.82714$ . (b2) Scaling behavior of charge susceptibilities near phase transition from IV to V driven by interaction.

entropy in the Luttinger liquid phases  $TTL_C$  and  $TTL_S$  are given by  $s_{L1} = \pi T_{L1}/3v_c$  and  $s_{L2} = \pi T_{L2}/3v_s$ , respectively. Therefore, through an interaction-driven refrigeration cycle near phase transitions from II to IV and from V to IV in the T-u plane, we can show that the reachable minimum temperatures are given by

$$\frac{T_{c1}^{1/2}}{T_{L1}} = \frac{\pi^{1/2} [\varepsilon_1^{00}(0)/2]^{1/2}}{3\lambda_1 v_c \sigma_1(0)},\tag{7}$$

$$\frac{T_{c2}^{1/2}}{T_{L2}} = \frac{\pi^{1/2} [-\kappa^{00}(\pi)/2]^{1/2}}{3\lambda_1 v_s \rho(\pi)},\tag{8}$$

respectively. The minimum temperature in the T-u plane is governed by the relation  $\alpha_u 1u/T \approx 1.3117$  [62]. We remark that efficient cooling in lattice is a significant experimental challenge in ultracold atomic gases, the lack of which poses as a roadblock for realizing some exotic quantum phases.

On the other hand, the other two relations in Eqs. (6) provide essential insights for charge (IV-V) and spin (II-IV) phase transitions, respectively. Using these, we find two useful relations among the parameters  $\alpha_{u,\mu,B}$  in Eq. (3),

$$\frac{\alpha_u}{\alpha_u} = -\frac{\partial \mu}{\partial u'}, \quad \frac{\alpha_u}{\alpha_B} = -\frac{\partial B}{\partial u'}, \tag{9}$$

that provide us deep insights into the quantum criticality driven by dynamical interaction and external potentials. For example, Fig. 4(b1) shows the phase transition from phase IV to the Mott phase V in the  $\mu - u$  plane, where  $\frac{\partial \mu}{\partial u}$  is the slope along the transition line n=1. From Eq. (9) with fixed  $B_c=0.82714$  around  $u_c=1$ ,  $\mu_c=-0.8272$  in Fig. 4(b1), we may numerically get  $\alpha_u \approx -1.9627$ . With this and using the scaling form of free energy given in Eq. (2), we can obtain the scaling behavior of the compressibility in terms of u, which is in excellent agreement with numerical calculation from TBA equations; see Fig. 4(b2).

Summary. We have presented rigorous results of the 1D repulsive Hubbard model. We focus on the interaction-driven quantum criticality which has been largely ignored in previous studies. We studied the fractional excitations from which the SILL regime is identified and carefully investigated. We introduced several contact susceptibilities and show how they provide crucial insights into the system. Finally, we proposed a quantum cooling scheme based on the interaction-driven refrigeration cycle, which can potentially

open up avenues of research in reaching unprecedented low temperatures in lattice quantum gases. We note that some of the key concepts developed here will hold true in higher dimensions.

Acknowledgments. J.J.L. and X.W.G. are supported by the NSFC key Grant No. 12134015 and the NSFC Grants No. 11874393 and No. 12121004. H.P. acknowledges support from the US NSF (Grant No. PHY-2207283) and the Welch Foundation (Grant No. C-1669).

- [1] E. H. Lieb and F. Y. Wu, Phys. Rev. Lett. 20, 1445 (1968).
- [2] E. H. Lieb and F. Wu, Physica A 321, 1 (2003).
- [3] T. Giamarchi, *Quantum Physics in One Dimension* (Oxford Science Publications, New York, 2004).
- [4] A. Imambekov, T. L. Schmidt, and L. I. Glazman, Rev. Mod. Phys. 84, 1253 (2012).
- [5] F. H. L. Essler, H. Frahm, F. Göhmann, A. Klümper, and V. E. Korepin, *The One-Dimensional Hubbard Model* (Cambridge University Press, Cambridge, UK, 2005).
- [6] M. Boll, T. A. Hilker, G. Salomon, A. Omran, J. Nespolo, L. Pollet, I. Bloch, and C. Gross, Science 353, 1257 (2016).
- [7] T. A. Hilker, G. Salomon, F. Grusdt, A. Omran, M. Boll, E. Demler, I. Bloch, and C. Gross, Science 357, 484 (2017).
- [8] J. Vijayan, P. Sompet, G. Salomon, J. Koepsell, S. Hirthe, A. Bohrdt, F. Grusdt, I. Bloch, and C. Gross, Science 367, 186 (2020).
- [9] B. M. Spar, E. Guardado-Sanchez, S. Chi, Z. Z. Yan, and W. S. Bakr, Phys. Rev. Lett. 128, 223202 (2022).
- [10] V. Ya. Krivnov and A. A. Ovchinnikov, Zh. Eksp. Teor. Fiz. 67, 1568 (1974) [Sov. Phys. JETP 40, 781 (1975)].
- [11] N. M. Bogoliubov and V. E. Korepin, Int. J. Mod. Phys. B 03, 427 (1989).
- [12] F. Woynarovich and K. Penc, Z. Phys. B 85, 269 (1991).
- [13] K.-J.-B. Lee and P. Schlottmann, Phys. Rev. B 38, 11566 (1988).
- [14] F. Woynarovich, J. Phys. C 16, 6593 (1983).
- [15] P. D. Sacramento, J. Phys.: Condens. Matter 7, 143 (1995).
- [16] F. H. L. Essler and V. E. Korepin, Nucl. Phys. B 426, 505 (1994).
- [17] P. Fulde and R. A. Ferrell, Phys. Rev. 135, A550 (1964).
- [18] A. I. Larkin and Y. N. Ovchinnikov, Zh. Eksp. Teor. Fiz. 47, 1136 (1964).
- [19] K. Yang, Phys. Rev. B 63, 140511(R) (2001).
- [20] M. Tezuka and M. Ueda, Phys. Rev. Lett. 100, 110403 (2008).
- [21] A. E. Feiguin and F. Heidrich-Meisner, Phys. Rev. B 76, 220508(R) (2007).
- [22] J. Kajala, F. Massel, and P. Törmä, Phys. Rev. A 84, 041601(R) (2011).
- [23] S. Cheng, Y.-C. Yu, M. T. Batchelor, and X.-W. Guan, Phys. Rev. B 97, 121111(R) (2018).
- [24] S. Cheng, Y.-Z. Jiang, Y.-C. Yu, M. T. Batchelor, and X.-W. Guan, Nucl. Phys. B 929, 353 (2018).
- [25] M. A. Cazalilla, M. A. Cazalilla, T. Giamarchi, E. Orignac, and M. Rigol, Rev. Mod. Phys. 83, 1405 (2011).
- [26] X. W. Guan, M. T. Batchelor, and C. Lee, Rev. Mod. Phys. 85, 1633 (2013).
- [27] M. T. Batchelor, and A Foerster, J. Phys. A: Math. Theor. 49, 173001 (2016).

- [28] S. I. Mistakidis, A. G. Volosniev, R. E. Barfknecht, T. Fogarty, T. Busch, A. Foerster, P. Schmelcher, and N. T. Zinner, arXiv:2202.11071.
- [29] T. Kinoshita, T. Wenger, and D. S. Weiss, Nature 440, 900 (2006).
- [30] T. Langen, S. Erne, R. Geiger, B. Rauer, T. Schweigler, M. Kuhnert, W. Rohringer, I. E. Mazets, T. Gasenzer, and J. Schmiedmyer, Science 348, 207 (2015).
- [31] M. Schemmer, I. Bouchoule, B. Doyon, and J. Dubail, Phys. Rev. Lett. **122**, 090601 (2019).
- [32] J. M. Wilson, N. Malvania, Y. Le, Y. Zhang, M. Rigol, and D. S. Weiss, Science 367, 1461 (2020).
- [33] B. Yang, Y.-Y. Chen, Y. G. Zheng, H. Sun, H. N. Dai, X.-W. Guan, Z. S. Yuan, and J.-W. Pan, Phys. Rev. Lett. 119, 165701 (2017).
- [34] T. L. Yang, P. Grišins, Y. T. Chang, Z. H. Zhao, C. Y. Shih, T. Giamarchi, and R. G. Hulet, Phys. Rev. Lett. 121, 103001 (2018).
- [35] F. Meinert, M. Panfil, M. J. Mark, K. Lauber, J. S. Caux, and H. C. Nägerl, Phys. Rev. Lett. 115, 085301 (2015).
- [36] X. B. Zhang, Y. Y. Chen, L. X. Liu, Y. I. Deng, and X.-W. Guan, Natl. Sci. Rev. 9, nwac027 (2022).
- [37] E. Haller, M. Gustavsson, M. J. Mark, J. G. Danzl, R. Hart, G. Pupillo, and H. C. Nägerl, Science 325, 1224 (2009).
- [38] W. Kao, K. Y. Li, K. Y. Lin, S. Gopalakrishnan, and B. L. Lev, Science 371, 296 (2021).
- [39] Y. T. Chang, R. Senaratne, D. Cavazos-Cavazos, and R. G. Hulet, Phys. Rev. Lett. **125**, 263402 (2020).
- [40] D. J. M. Ahmed-Braun, K. G. Jackson, S. Smale, C. J. Dale, B. A. Olsen, S. J. J. M. F. Kokkelmans, P. S. Julienne, and J. H. Thywissen, Phys. Rev. Res. 3, 033269 (2021).
- [41] K. G. Jackson, C. J. Dale, J. Maki, K. G. S. Xie, B. A. Olsen, D. J. M. Ahmed-Braun, S. Zhang, and J. H. Thywissen, Phys. Rev. X 13, 021013 (2023).
- [42] G. Pagano, M. Mancini, G. Cappellini, P. Lombardi, F. Schäfer, H. Hu, X.-J. Liu, J. Catani, C. Sias, M. Inguscio, and L. Fallani, Nat. Phys. 10, 198 (2014).
- [43] B. Song, Y. Yan, C. He, Z. Ren, Q. Zhou, and G. B. Jo, Phys. Rev. X 10, 041053 (2020).
- [44] X.-W. Guan and P. He, Rep. Prog. Phys. 85, 114001 (2022).
- [45] H. Chen and K. Yang, Phys. Rev. B 85, 195113 (2012).
- [46] W. Li, D. N. Sheng, C. S. Ting, and Y. Chen, Phys. Rev. B 90, 081102(R) (2014).
- [47] H. Pan and S. Das Sarma, Phys. Rev. Lett. 127, 096802 (2021).
- [48] F. D. M. Haldane, J. Phys. C: Solid State Phys. 14, 2585 (1981).
- [49] A. Recati, P. O. Fedichev, W. Zwerger, and P. Zoller, Phys. Rev. Lett. 90, 020401 (2003).

- [50] J. Y. Lee, X.-W. Guan, K. Sakai, and M. T. Batchelor, Phys. Rev. B **85**, 085414 (2012).
- [51] M. Mestyán, B. Bertini, L. Piroli, and P. Calabrese, Phys. Rev. B 99, 014305 (2019).
- [52] O. I. Pâţu, A. Klümper, and A. Foerster, Phys. Rev. B 101, 035149 (2020).
- [53] R. Senaratne, D. Cavazos-Cavazos, S. Wang, F. He, Y.-T. Chang, A. Kafle, H. Pu, X.-W. Guan, and R. G. Hulet, Science 376, 1305 (2022).
- [54] D. Cavazos-Cavazos, R. Senaratne, A. Kafle, and R. G. Hulet, arXiv:2210.06306.
- [55] G. A. Fiete and L. Balents, Phys. Rev. Lett. 93, 226401 (2004).
- [56] G. A. Fiete, Rev. Mod. Phys. 79, 801 (2007).
- [57] V. V. Cheianov and M. B. Zvonarev, Phys. Rev. Lett. 92, 176401 (2004).
- [58] S. Tan, Ann. Phys. (NY) 323, 2952 (2008).

- [59] S. Zhang and A. J. Leggett, Phys. Rev. A 79, 023601 (2009).
- [60] C. N. Yang, Phys. Rev. Lett. 63, 2144 (1989).
- [61] C. N. Yang and S. C. Zhang, Mod. Phys. Lett. B 04, 759 (1990).
- [62] See Supplemental Material at http://link.aps.org/supplemental/ 10.1103/PhysRevB.107.L201103 in which we present some key derivations of the results on the fractional excitations, SILL correlation functions, interaction driven criticality, and quantum cooling for the 1D repulsive Hubbard model. The Supplemental Material also contains Ref. [63].
- [63] N. Mohankumar, Comput. Phys. Commun. 176, 665 (2007).
- [64] H. A. Bethe, Z. Phys. 71, 205 (1931).
- [65] M. Takahashi, Prog. Theor. Phys. 47, 69 (1972).
- [66] C. N. Yang and C. P. Yang, J. Math. Phys. 10, 1115 (1969).
- [67] Y.-C. Yu, S.-Z. Zhang, and X.-W. Guan, Phys. Rev. Res. 2, 043066 (2020).